Decoupling mesoscale functional response in PLZT across the ferroelectric – relaxor phase transition with contact Kelvin probe force microscopy and machine learning

Sabine M. Neumayer[1,2]*, Liam Collins[1], Rama Vasudevan[1], Christopher Smith[1], Suhas Somnath[1], Vladimir Ya. Shur[3], Stephen Jesse[1], Andrei L. Kholkin[3,4], Sergei V. Kalinin[1], Brian J. Rodriguez[2]

[1] Center for Nanophase Materials Sciences, Oak Ridge National Laboratory, 1 Bethel Valley Rd. Oak Ridge, TN 37831, USA

[2] School of Physics, University College Dublin, Belfield 4, Ireland

[3] School of Natural Sciences and Mathematics, Ural Federal University, 620000 Ekaterinburg, Russia

[4] Department of Physics & CICECO- Aveiro Institute of Materials, 3810-193 Aveiro, Portugal

* neumayersm@ornl.gov

Abstract

Relaxor ferroelectrics exhibit a range of interesting material behavior including high electromechanical response, polarization rotations as well as temperature and electric field-driven phase transitions. The origin of this unusual functional behavior remains elusive due to limited knowledge on polarization dynamics at the nanoscale. Piezoresponse force microscopy and associated switching spectroscopy provide access to local electromechanical properties on the micro- and nanoscale, which can help to address some of these gaps in our knowledge. However, these techniques are inherently prone to artefacts caused by signal contributions emanating from electrostatic interactions between tip and sample. Understanding functional

behavior of complex, disordered systems like relaxor materials with unknown electromechanical properties therefore requires a technique that allows to distinguish between electromechanical and electrostatic response. Here, contact Kelvin probe force microscopy (cKPFM) is used to gain insight into the evolution of local electromechanical and capacitive properties of a representative relaxor material lead lanthanum zirconate across the phase transition from a ferroelectric to relaxor state. The obtained multidimensional data set was processed using an unsupervised machine learning algorithm to detect variations in functional response across the probed area and temperature range. Further analysis showed formation of two separate cKPFM response bands below 50°C, providing evidence for polarization switching. At higher temperatures only one band is observed, indicating an electrostatic origin of the measured response. In addition, from the cKPFM data qualitatively extracted junction potential difference, becomes independent of the temperature in the relaxor state. The combination of this multidimensional voltage spectroscopy technique and machine learning allows to identify the origin of the measured functional response and to decouple ferroelectric from electrostatic phenomena necessary to understand the functional behavior of complex, disordered systems like relaxor materials.

Keywords

Relaxor ferroelectric, phase transition, lead lanthanum zirconium titanate, contact Kelvin probe force microscopy, piezoresponse force microscopy, machine learning, k-means clustering

Introduction

The remarkably high electrostrictive response observed in relaxor ferroelectrics combined with their large dielectric and electro-optic constants have awoken significant interest in these materials for applications such as electromechanical transducers, capacitive energy storage and electro-optic modulators.[1–6] Moreover, phase transitions between ferroelectric and relaxor states yield additional functionality in terms of pyroelectric energy harvesting or temperature dependent electromechanical sensing, for which lead lanthanum zirconate titanate (PLZT) is a highly suitable material as it exhibits low phase transition temperatures near room temperature and large electrostriction.[2,3,5,7,8] While the underlying physical phenomena warrant high scientific interest in itself, knowledge on the functional material response to an electric field at operating temperatures is also key to device design. Understanding the overall macroscopic behavior of these heterogeneous materials as well as micro- and nanoscale applications necessitate assessment of local characteristics, which is widely studied using piezoresponse force microscopy (PFM) and related switching spectroscopy techniques.[9–13]

PFM is based on detecting cantilever oscillation corresponding to periodic sample deformation in response to an alternating voltage (V_{ac}) due to the converse piezoelectric effect.[14] However, V_{ac} excitation also leads to detection of electrostatic forces between tip and sample, which can contribute to the measured signal in PFM.[15–18] The high direct voltages (V_{dc}) pulses that are applied in switching spectroscopy to induce switching can prompt charge injection and other changes in the junction contact potential difference (jCPD), which directly effects electrostatic forces even between pulses in the absence of V_{dc}. Consequently, measured PFM hysteresis loops can solely emanate from changes in electrostatic forces, imposing further challenges on characterization of relaxor materials. Even more so as relaxors often exhibit peculiarities in

hysteresis loops even in the ferroelectric state, especially near phase transition temperatures.[19] Gaining insight into the evolution of genuine electromechanical behavior of a PLZT relaxor material across the ferroelectric - relaxor phase transition necessitates a more elaborate approach.

In this work, contact mode Kelvin probe force microscopy (cKPFM)[15,20] spectroscopy was performed on PLZT of 8/65/35 composition across a temperature range from 5°C to 95°C. The surface area comprises multiple grains (Figure 1(a)). This technique has been proven useful to study the functional behavior of ferroelectric and non-ferroelectric materials, especially under variation of factors like sample thickness as well as internal and external screening conditions.[15,16,21–24] However, this technique has not been applied to study phase transitions in relaxors yet.

Relaxor ferroelectrics provide a model material system where the electromechanical response is typically high, the transition temperature is experimentally accessible and a range of polarization states can potentially be favored as field induced polarization can be large and long-lived.[13] The cKPFM technique harnesses electrostatic forces by controlling them through a V_{dc} sweep applied sequentially during read steps in multiple cycles. For clarity, a schematic depiction of the sequence of voltage pulses applied in cKPFM is illustrated in Figure 1(b), whereas the experimentally applied V_{dc} waveform is shown in the supplementary information Figure SI1. Similar to conventional switching spectroscopy, switching is induced by a train of V_{dc} write pulses of increasing amplitude in a triangular waveform envelope. However, instead of V_{dc} = 0 V during all read steps between write pulses, in cKPFM multiple cycles are applied during which a read voltage is successively increased for each cycle from negative to 0 V to positive voltages (see waveform depicted in SI Figure 1). The cycle at 0 V corresponds to conventional PFM switching

spectroscopy. Additional V_{ac} excitation in a frequency band around the contact resonance monitors the resulting response signal of electromechanical and electrostatic origin.[25] From the response at each read and write voltage, the number of polarization states and effect of write pulses on jCPD and capacitance gradient can be obtained. The response measured during the read step at 0 V corresponds to the signal obtained in classical PFM spectroscopy modes.

Results and discussion

For macroscopic pre-characterization of the sample, dielectric measurements were performed. As shown in SI Figure SI2, at room temperature there is only a small frequency dispersion of the permittivity, typical for conventional ferroelectrics. However, the frequency dispersion becomes more pronounced with increasing temperature. The melting temperature T_m that indicates transition to the paraelectric state corresponds to the position of the dielectric maximum and shows a frequency dependent shift, which is a signature of relaxor ferroelectrics.[2] These characteristics suggest that the ceramic exhibits electromechanical properties between a classical ferroelectric material and a relaxor within the temperature range of 5°C to 95°C used in cKPFM studies. T_m was determined to be 107 ± 2°C at 1 kHz, while the freezing temperature T_f at which transition between ferroelectric and relaxor state occurs was found to be 47 ± 2°C. The relaxor phase characteristically shows high dielectric constants due to interactions between randomly oriented polar nanodomains but small remanent polarization.[2,7] With decreasing temperature, the interaction radius between nanodomains increases which leads to coalescence into macroscopic polar clusters with large remanent polarization, marking the ferroelectric state.

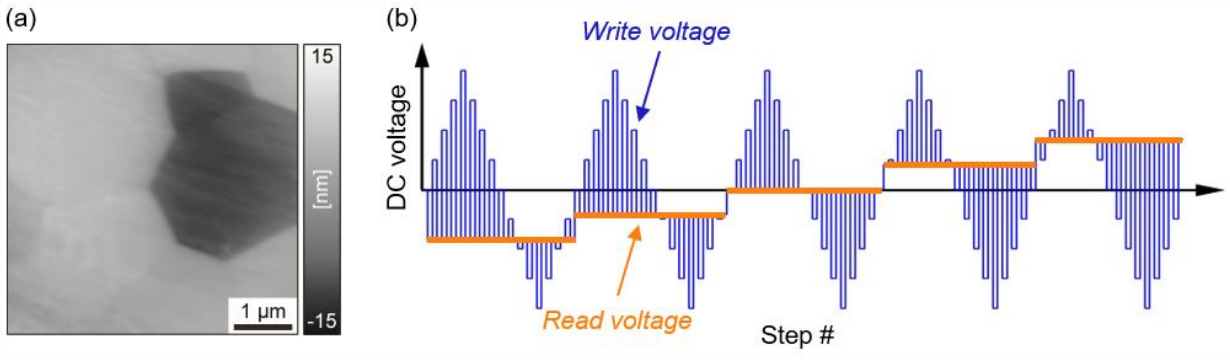

Figure 1: (a) Topography image of PLZT surface comprising several grains. (b) Scheme of voltage waveforms applied in cKPFM. A DC read voltage is applied between write pulses and varied in multiple cycles.

cKPFM spectroscopy was applied across several grains in maps of 10×10 pixels. The applied voltage waveform, as depicted in SI Figure S1 consists of 720 steps for each of those 100 pixels and 7 temperature steps, leading to a total of 504 000 data points. Given the amount of data points and general difficulties to find statistical metrics to determine the onset of phase transitions, clustering have been applied to the data as these algorithms encode information on the functional response in correlation with the phase status. To get an overview on phase transition temperatures (as indicated by a change in cKPFM response) and detect whether there are significant local variations between grains, k-means clustering was performed on the whole data set, i.e. the response measured at each pixel during the applied voltage waveform for all temperature steps. This unsupervised machine learning algorithm finds similarities in data sets and groups the data points into clusters accordingly. The centers of each cluster for all waveform steps are the obtained centroids and correspond to the mean value of the measured response (y-axis) for each step of the voltage waveform (x-axis). For each temperature step, each pixel is assigned to the cluster whose

centroid is in closest proximity to the measured response for each temperature step. In k-means clustering, the number of clusters can be chosen. In this case, 3 clusters are identified to represent the data best. The centroids of the three clusters for each step of the voltage waveform and corresponding maps of 10×10 pixels illustrating the spatial distribution of clusters for each temperature step are shown in Figure 2(a) and (b), respectively. The centroids provide a measure for the average response of each cluster for each step of the applied waveform. Therefore, the maps highlight how electromechanical behavior varies within the map and with temperature. With the applied sequence of voltage pulses (SI Figure SI 1) in mind and considering that read and write pulses of different amplitude are applied alternatingly, we can discern interesting features of the centroids of the three clusters: Cluster 0 response shows strong relaxation between read and write pulses, as indicated by the nearly completely color filled area within the curve envelope. Cluster 1, however, shows less difference between read and write steps, pointing to a more stable response induced by write pulses, which is usually associated with a remanent polarization. The electromechanical behavior in cluster 2 appears as intermediate state between cluster 0 and cluster 1. All three cases exhibit asymmetries between positive and negative write voltages. The k-means maps in Figure 2(b) show that the obtained response varies with temperature but is nearly uniform within the 10×10 maps. Moreover, a strong change in electromechanical response from cluster 1 to mainly cluster 0 occurs between 35°C and 50°C, after which cluster 0 dominates, marking the phase transition between ferroelectric and relaxor states. Intermediate response as indicated by cluster 2 assignment occurs at a few pixels mainly during 35°C and 50°C close to the phase transition temperature. It is highly unexpected that response measured at the lowest temperature of 5°C shows the same intermediate behavior for the whole map. However, in an experiment

preceding the 5°C measurement, the sample was heated up to 60°C and might not have fully cooled down within the 30 min waiting time at 5°C before the cKPFM map was acquired.

In general, electrostatic forces in cKPFM are sensitive to the local topography due to changes in the tip – sample contact.[26] The response measured at concave surface areas (e.g. at grain boundaries) can therefore be higher than at convex locations. However, in our grid of 10x10 points over grains of several μm^2 in size, the tip is mostly situated within the grains, where the roughness of the polished surface is equal for all grains. Moreover, the absence of significant, reoccurring local response variations in Figure 2(b) indicates the measured cKPFM signal in this study is not strongly affected by topography.

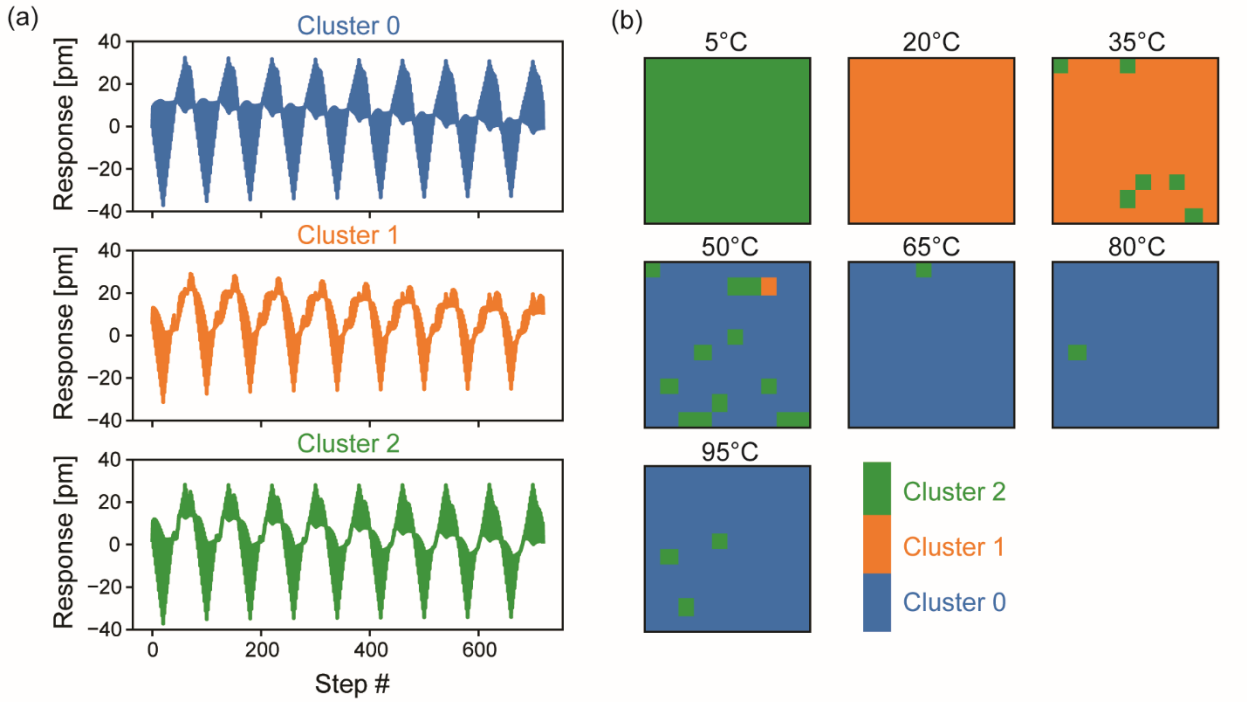

Figure 2: k-means clustering of cKPFM response for all 7 temperature steps. (a) Centroids of cKPFM response for each step of the applied voltage waveform depicted for all three clusters. (b) Corresponding maps of 10×10 pixels showing the cluster each pixel belongs to at each temperature step.

As the electromechanical response does not show substantial local variations, we average cKPFM response over the 10×10 pixels of each map in subsequent analysis. Figure 3(a) shows cKPFM diagrams obtained for each temperature step from 5°C to 95°C in intervals of 15°C. These graphs display the measured electromechanical response (y-axis) plotted vs. the read voltage (x-axis) for each write voltage step as indicated by colors. For example, the dark red line shows the response after the -45 V write step in each of the 9 cycles, which correspond to a certain read voltage. The y-intercept at 0 V corresponds to the PFM signal that is measured in classical switching spectroscopy, whereas the x-intercept provides a measure for the jCPD, similar to the contact potential difference in conventional, non-contact Kelvin probe force microscopy.

For temperatures up to 35°C, response curves after high positive (blue curves) and negative (red curves) write voltages form two separate bands, accompanied by transitions between those bands at low write voltages (green curves). The two distinct bands and transitions between them correspond to switching between two polarization states induced by V_{dc} write pulses. In previous observations by Balke *et al.*,[16] cKPFM response curves shape on ferroelectric lead zirconate titanate additionally showed a hysteresis, which can be attributed to the higher ratio between read and write voltages.

Starting from 50°C, cKPFM curves collapse into one continuous band, in agreement with k-means clustering and the T_f observed in macroscopic dielectric measurements that indicate transition from the ferroelectric to the relaxor state. The 3-dimensional graph in Figure 3(b) summarizes the temperature dependence of cKPFM response measured after +45 V (blue) and -

45 V (red) write pulses. While the red curve shows higher positive values than the blue curve in the ferroelectric state, a cross-over occurs after phase transition for temperatures >65°C with the blue curve showing higher positive response. The intermediate electromechanical behavior at 5°C manifests itself in a smaller distance between cKPFM bands and the slopes of the two bands significantly differ.

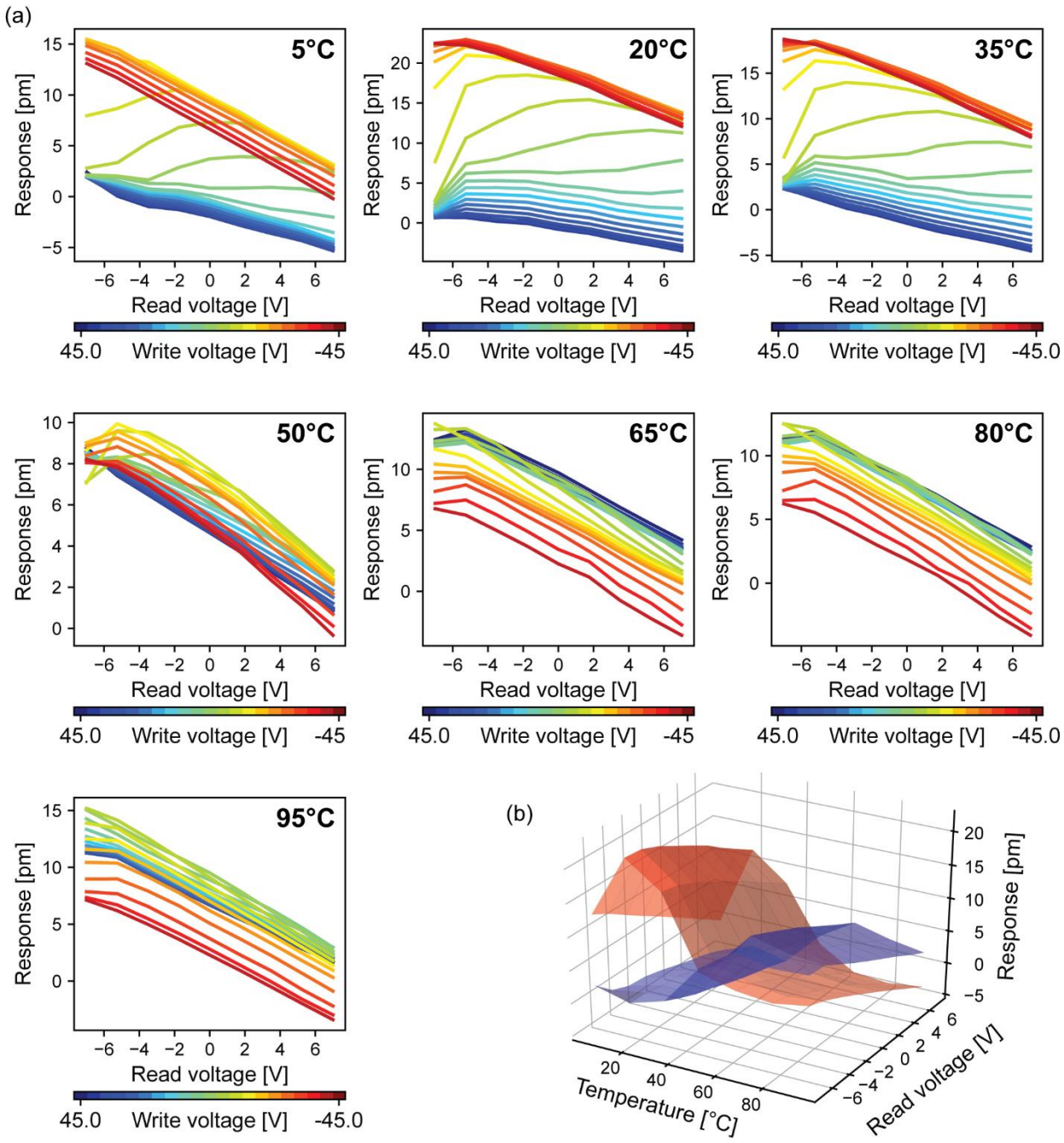

Figure 3: (a) Diagrams of cKPFM response plotted vs. read voltage for each write voltage step from +45 V to -45 V (color coded). (b) 3-dimensional representation of response after +45 V (blue) and -45 V (red) write pulses as a function of read voltage and temperature.

For comparison, the in-field (IF) and out-of-field (OOF) response extracted from the cycle at 0 V read voltage, is plotted vs. the write voltage in Figure 4 for all temperature steps. These loops are traditionally used in standard switching spectroscopy to characterize ferroelectric properties. As seen for the k-means cluster centroids, all IF and OOF loops exhibit a strong asymmetry between positive and negative write voltages. The loop area in IF and OOF response significantly decreases after phase transition due to the decrease in remanent polarization. For OOF loops, additionally a change in loop orientation from clockwise to counter-clockwise occurs, which is evidence for a change in the mechanism that predominantly contributes to the measured signal from ferroelectricity to electrostatics. Moreover, the OOF response is much lower after the phase transition.

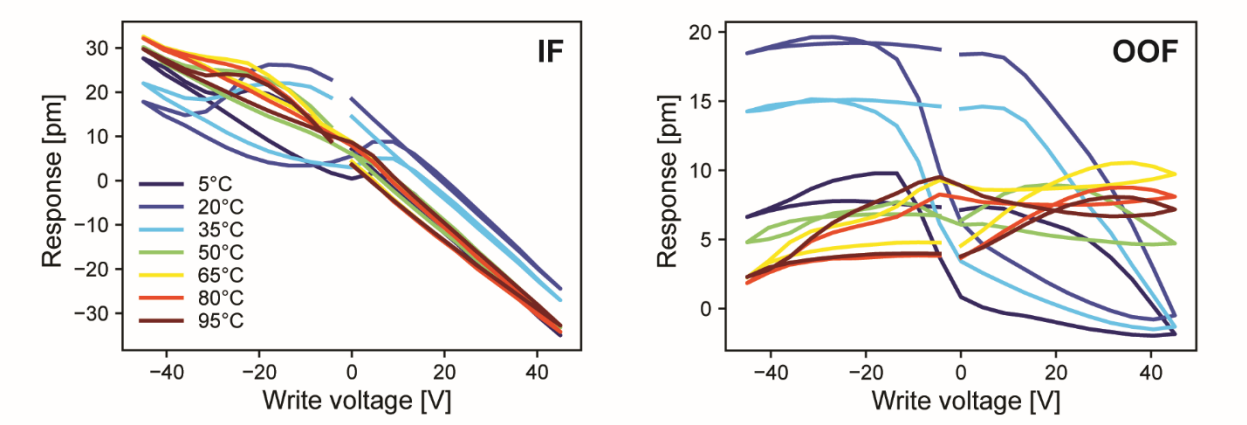

Figure 4: IF and OOF response loops measured during the 0 V read cycle at different temperature steps.

Linear fitting was applied to cKPFM curves within a read voltage range from -5.25 V to 7 V. The resulting fitting parameters slope, y-intercept and x-intercept as measure for the jCPD are

depicted in Figure 5 as a function of temperature for highest positive (+45 V) and negative (-45 V) write V_{dc} pulses as well as for 0 V. In the relaxor state at temperatures between 65°C and 95°C, jCPD, slope and y-intercept are nearly constant between 65°C and 95°C for +45 V, -45 V and 0 V. The obtained slope represents the quotient of capacitance gradient and stiffness of the tip – sample contact. The capacitance gradient is related to the tip – sample capacitor geometry as well as dielectric properties. The steeper negative slopes for -45 V compared to +45 V might originate from asymmetries in charge injection caused by favorable band bending for negative voltages, which can change dielectric properties. The slope most strongly varies for 0 V write biases, which indicates a band transition between the lower and the upper cKPFM bands with increasing write voltage. These band transitions are common at low write voltage steps where the read voltage dominates the response or near coercive voltages when switching occurs. For example, the positive slope values for the 0 V curve indicate a transition from the lower to the upper band. Corresponding to the previously discussed cross-over of cKPFM response (Figure 3(b)) and changes in OOF loop orientation (Figure 4), cross-overs are also evident for y-intercepts at +45 V and -45 V and consequently also the jCPD curves. This behavior is consistent considering that in the ferroelectric state, negative (positive) voltage pulses lead to more positive (negative) values for the jCPD due to the presence of polarization switching. However, above the phase transition, negative (positive) V_{dc} results in injection of negative (positive) charges. For 0 V, y-intercept and jCPD exhibits similar behavior as for +45 V, which is the preceding voltage polarity. Data extracted for low voltages following -45 V are comparable to -45 V curves (not shown).

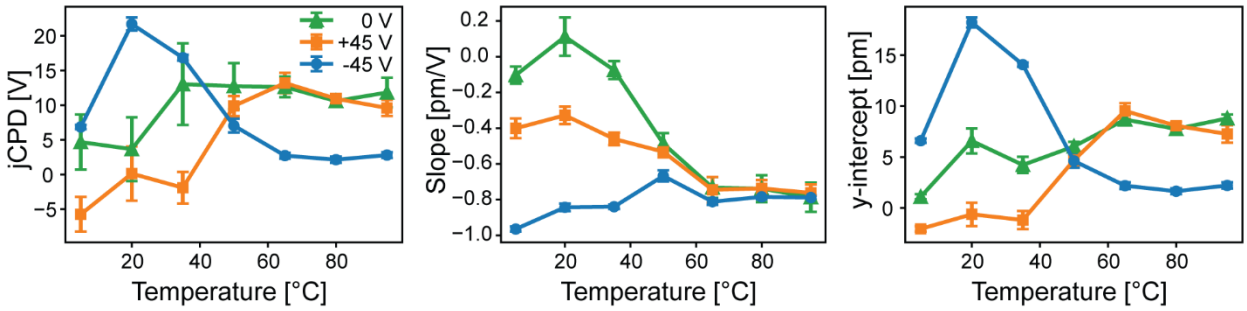

Figure 5: jCPD, slope and y-intercept averaged over the whole 10x10 map as a function of temperature.

Conclusions

In conclusion, cKPFM and k-means clustering are used to identify the origin of local functional response in PLZT across the transition from ferroelectric to relaxor state. K-means clustering of cKPFM data revealed that the phase transition occurs near 50°C for all grains, which in cKPFM analysis is manifested as collapsing bands in cKPFM response. Correspondingly, OOF hysteresis loops change orientation and show lower response, while IF loops before and after transition are similar. From cKPFM response, the extracted measure for jCPD as well as the slope and y-intercept are constant for the same write pulse in the relaxor state whereas pronounced temperature and write voltage dependence is observed before the phase transition. These findings yield insight into the development of local electromechanical and electrostatic response across the ferroelectric – relaxor transition temperature and aid interpretation of PFM and cKPFM data of similar materials.

Experimental

$Pb_{0.92}La_{0.08}(Zr_{0.65}Ti_{0.35})_{0.98}O_3$ (PLZT 8/65/35) relaxor ceramics were sintered using the hot pressing method. A platelet-shaped sample of 1.0 mm thickness and a surface area of ca. 3x3 mm^2 was polished to optical quality.

Macroscopic permittivity measurements were performed using an Agilent E4980 Precision LCR Meter connected to a home-built temperature stage with an Eurotherm temperature controller.

An Asylum Research Cypher atomic force microscopy equipped with a temperature stage was used for all measurements. Generation of the excitation signal and data acquisition was performed with National Instrument DAQ card and chassis, interfaced with LabView programs. A conductive Budgetsensor Multimode probe (nominal force constant = 3 N/m, nominal resonance frequency = 75 kHz was used. cKPFM maps of 10x10 pixels were obtained from the area depicted in Figure 1(a) upon varying the temperature from 5 °C to 95 °C in 7 steps. The cKPFM waveform (SI Figure 1) consists of 40 write steps between +/- 45 V and 9 read steps between +/- 7 V. For AC excitation, a signal of 3 V and a frequency band centered around the contact resonance was applied. The obtained response was fitted using a simple harmonic oscillator model to extract amplitude, phase, resonance frequency and Q- factor. Data processing and analysis was partially performed using pycroscopy.[27]

Acknowledgements

The authors would like to thank Prof. Andris Sternbergs from the Institute of Solid State Physics at University of Latvia (Riga), for providing PLZT samples. This work was conducted the Center for Nanophase Materials Sciences at Oak Ridge National Laboratory, which is a DOE Office of Science User Facility (CNMS2017-R49) and has emanated from research supported in part by a research grant from Science Foundation Ireland (SFI) under the US-Ireland R&D Partnership Programme Grant Number SFI/14/US/I3113. The scanning probe microscopy part of this work was supported by the U.S. Department of Energy, Office of Science, Basic Energy Sciences. VYS and ALK acknowledges the support by the Russian Foundation of Basic Research (Grant 16-02-00821-a).

Supporting information

Applied cKPFM voltage waveform, permittivity as function of temperature at different frequencies.

References

(1) Pirc, R.; Blinc, R.; Vikhnin, V. S. Effect of Polar Nanoregions on Giant Electrostriction and Piezoelectricity in Relaxor Ferroelectrics. *Phys. Rev. B - Condens. Matter Mater. Phys.* **2004**, *69* (21), 212105-1–21210-4.

(2) Samara, G. A. The Relaxational Properties of Compositionally Disordered ABO_3 Perovskites. *J. Phys. Condens. Matter* **2003**, *15* (9), R367–R411.

(3) Lozinski, A.; Wang, F.; Uusimäki, A.; Leppävuori, S. PLZT Thick Films for Pyroelectric Sensors. *Meas. Sci. Technol.* **1997**, *8*, 33–37.

(4) Hu, Z.; Ma, B.; Liu, S.; Narayanan, M.; Balachandran, U. Relaxor Behavior and Energy Storage Performance of Ferroelectric PLZT Thin Films with Different Zr/Ti Ratios. *Ceram. Int.* **2014**, *40* (1 PART A), 557–562.

(5) Lee, F. Y.; Goljahi, S.; McKinley, I. M.; Lynch, C. S.; Pilon, L. Pyroelectric Waste Heat Energy Harvesting Using Relaxor Ferroelectric 8/65/35 PLZT and the Olsen Cycle. *Smart Mater. Struct.* **2012**, *21* (2), 025021.

(6) Vasudevan, R. K.; Zhang, S.; Ding, J.; Okatan, M. B.; Jesse, S.; Kalinin, S. V.; Bassiri-Gharb, N. Mesoscopic Harmonic Mapping of Electromechanical Response in a Relaxor Ferroelectric. *Appl. Phys. Lett.* **2015**, *106* (22), 222901.

(7) Lee, F. Y.; Jo, H. R.; Lynch, C. S.; Pilon, L. Pyroelectric Energy Conversion Using PLZT Ceramics and the Ferroelectric–ergodic Relaxor Phase Transition. *Smart Mater. Struct.* **2013**, *22* (2), 025038.

(8) Sebald, G.; Guiffard, B.; Seveyrat, L.; Benayad, A.; Lebrun, L.; Pruvost, S.; Guyomar, D. Electrocaloric Effect In Relaxor Ferroelectric Ceramics and Single Crystals. In *15th IEEE International Symposium on the Applications of Ferroelectrics*; 2006; 152–155.

(9) Vasudevan, R. K.; Zhang, S.; Baris Okatan, M.; Jesse, S.; Kalinin, S. V.; Bassiri-Gharb, N. Multidimensional Dynamic Piezoresponse Measurements: Unraveling Local Relaxation Behavior in Relaxor-Ferroelectrics via Big Data. *J. Appl. Phys.* **2015**, *118* (7), 072003.

(10) Brewer, S.; Deng, C.; Callaway, C.; Kalinin, S. V.; Vasudevan, R. K.; Bassiri-Gharb, N. Piezoelectric Response Enhancement in the Proximity of Grain Boundaries of Relaxor-Ferroelectric Thin Films. *Appl. Phys. Lett.* **2016**, *108* (24), 242908.

(11) Kholkin, A.; Morozovska, A.; Kiselev, D.; Bdikin, I.; Rodriguez, B.; Wu, P.; Bokov, A.; Ye, Z. G.; Dkhil, B.; Chen, L. Q.; Kosec, M.; Kalinin, S. V. Surface Domain Structures and Mesoscopic Phase Transition in Relaxor Ferroelectrics. *Adv. Funct. Mater.* **2011**, *21* (11), 1977–1987.

(12) Shvartsman, V. V; Kholkin, A. L. Polar Structures of $PbMg_{1/3}Nb_{2/3}O_3$-$PbTiO_3$ Relaxors: Piezoresponse Force Microscopy Approach. *J. Adv. Dielectr.* **2012**, *02* (02), 1241003.

(13) Shvartsman, V. V.; Dkhil, B.; Kholkin, A. L. Mesoscale Domains and Nature of the Relaxor State by Piezoresponse Force Microscopy. *Annu. Rev. Mater. Res.* **2013**, *43* (1), 423–449.

(14) Balke, N.; Bdikin, I.; Kalinin, S. V.; Kholkin, A. L. Electromechanical Imaging and Spectroscopy of Ferroelectric and Piezoelectric Materials: State of the Art and Prospects for the Future. *J. Am. Ceram. Soc.* **2009**, *92* (8), 1629–1647.

(15) Balke, N.; Maksymovych, P.; Jesse, S.; Kravchenko, I. I.; Li, Q.; Kalinin, S. V. Exploring Local Electrostatic Effects with Scanning Probe Microscopy : Implications for Piezoresponse Force Microscopy and Triboelectricity. *ACS Nano* **2014**, *8* (10), 10229–10236.

(16) Balke, N.; Maksymovych, P.; Jesse, S.; Herklotz, A.; Tselev, A.; Eom, C.; Kravchenko, I. I.; Yu, P.; Kalinin, S. V. Differentiating Ferroelectric and Nonferroelectric Electromechanical Effects with Scanning Probe Microscopy. *ACS Nano* **2015**, *9* (6), 6484–6492.

(17) Balke, N.; Jesse, S.; Carmichael, B.; Okatan, M.B.; Kravchenko, I.I.; Kalinin, S. V.; Tselev, A. Quantification of Probe-Sample Electrostatic Forces with Dynamic Atomic Force Microscopy. *Nanotechnology* **2017**, 28 (6), 065704.

(18) Vasudevan, R. K.; Balke, N.; Maksymovych, P.; Jesse, S.; Kalinin, S. V. Ferroelectric or Non-Ferroelectric: Why so Many Materials Exhibit "Ferroelectricity" on the Nanoscale. *Appl. Phys. Rev.* **2017**, *4* (2), 021302.

(19) Vasudevan, R. K.; Khassaf, H.; Cao, Y; Zhang, S.; Tselev, A; Carmichael, B.; Okatan, M. B.; Jesse, S.; Chen, L.Q.; Alpay, S.P.; Kalinin, S. V.; Bassiri-Gharb, N. Acoustic Detection of Phase Transitions at the Nanoscale. *Adv. Funct. Mater.* **2015**, *26* (4), 478–486.

(20) Balke, N.; Maksymovych, P.; Jesse, S.; Herklotz, A.; Tselev, A.; Eom, C.; Kravchenko, I. I.; Yu, P.; Kalinin, S. V. Differentiating Ferroelectric and Nonferroelectric Effects with Scanning Probe Microscopy. *ACS Nano* **2015**, *9* (6), 6484–6492.

(21) Neumayer, S. M.; Ievlev, A. V; Collins, L.; Vasudevan, R.; Baghban, M. A.; Ovchinnikova, O.; Jesse, S.; Gallo, K.; Rodriguez, B. J.; Kalinin, S. V. Surface Chemistry Controls Anomalous Ferroelectric Behavior in Lithium Niobate. *ACS Appl. Mater. Interfaces* **2018**, *10*, 29153–29160.

(22) Yang, S. M.; Morozovska, A. N.; Kumar, R.; Eliseev, E. A.; Cao, Y.; Mazet, L.; Balke, N.; Jesse, S.; Vasudevan, R. K.; Dubourdieu, C.; Kalinin, S. V. Mixed Electrochemical–ferroelectric States in Nanoscale Ferroelectrics. *Nat. Phys.* **2017**, *13*, 812-818.

(23) Ganeshkumar, R.; Somnath, S.; Cheah, C. W.; Jesse, S.; Kalinin, S. V; Zhao, R. Decoding Apparent Ferroelectricity in Perovskite Nano Fibers. *J. Appl. Mater. Interfaces* **2017**, *9*, 42131–42138.

(24) Hu, Q.; Bian, J.; Zelenovskiy, P. S.; Tian, Y.; Jin, L.; Wei, X.; Xu, Z.; Shur, V. Y. Symmetry Changes during Relaxation Process and Pulse Discharge Performance of the $BaTiO_3$-$Bi(Mg_{1/2}Ti_{1/2})O_3$ Ceramic. *J. Appl. Phys.* **2018**, *124* (5), 054101.

(25) Jesse, S.; Vasudevan, R. K.; Collins, L.; Strelcov, E.; Okatan, M. B.; Belianinov, A.; Baddorf, A. P.; Proksch, R.; Kalinin, S. V. Band Excitation in Scanning Probe Microscopy: Recognition and Functional Imaging. *Annu. Rev. Phys. Chem.* **2014**, *65*, 519–536.

(26) Balke, N.; Jesse, S.; Carmichael, B.; Okatan, M. B.; Kravchenko, I. I.; Kalinin, S. V; Tselev, A. Quantification of In-Contact Probe-Sample Electrostatic Forces with Dynamic Atomic Force Microscopy. *Nanotechnology* **2017**, *28* (6), 065704.

(27) Somnath, Suhas, Chris R. Smith, Nouamane Laanait, and Stephen Jesse. Pycroscopy. *Web*, Computer software. Vers. 0.60.0. Oak Ridge National Laboratory, **01 June 2016**. <https://pycroscopy.github.io/pycroscopy/about.html>.

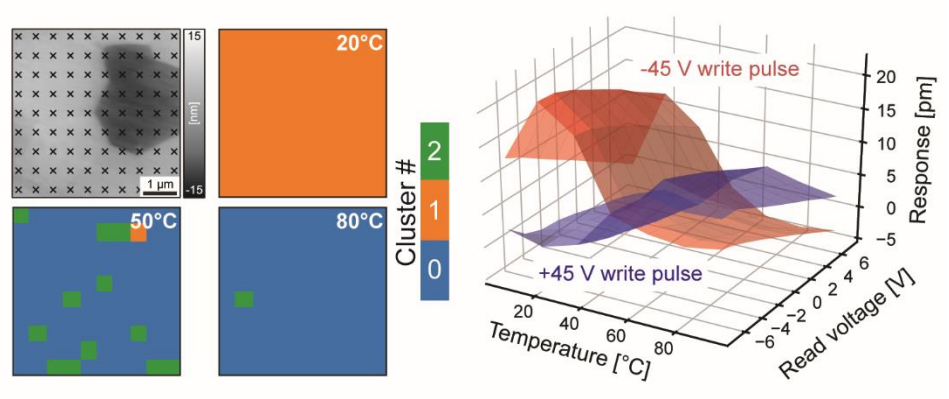

Table of contents figure